Published in final edited form as:
Cancer Discov. 2013 May ; 3(5): 520–533. doi:10.1158/2159-8290.CD-12-0531.

Relief of feedback inhibition of HER3 transcription by RAF and MEK inhibitors attenuates their antitumor effects in BRAF mutant thyroid carcinomas

Cristina Montero-Conde[1], **Sergio Ruiz-Llorente**[1,#], **Jose M. Dominguez**[1,#], **Jeffrey A. Knauf**[1], **Agnes Viale**[2], **Eric J. Sherman**[3], **Mabel Ryder**[1,3], **Ronald A. Ghossein**[4], **Neal Rosen**[3,5], and **James A. Fagin**[1,3,6]

[1]Human Oncology and Pathogenesis Program, Memorial Sloan-Kettering Cancer Center, New York, NY 10065, USA

[2]Sloan Kettering Institute, Memorial Sloan-Kettering Cancer Center, New York, NY 10065, USA

[3]Department of Medicine, Memorial Sloan-Kettering Cancer Center, New York, NY 10065, USA

[4]Department of Pathology, Memorial Sloan-Kettering Cancer Center, New York, NY 10065, USA

[5]Molecular Pharmacology and Chemistry Program, Memorial Sloan-Kettering Cancer Center, New York, NY 10065, USA

Abstract

The RAF inhibitor vemurafenib (PLX4032) increases survival in patients with *BRAF*-mutant metastatic melanoma, but has limited efficacy in patients with colorectal cancers. Thyroid cancer cells are also comparatively refractory to RAF inhibitors. By contrast to melanomas, inhibition of MAPK signaling by vemurafenib is transient in thyroid and colorectal cancer cells. The rebound in ERK in thyroid cells is accompanied by increased HER3 signaling caused by induction of HER3 transcription through decreased promoter occupancy by the transcriptional repressors CtBP1 and 2, and by autocrine secretion of neuregulin-1. The HER kinase inhibitor lapatinib prevents MAPK rebound and sensitizes BRAF-mutant thyroid cancer cells to RAF or MEK inhibitors. This provides a rationale for combining ERK pathway antagonists with inhibitors of feedback-reactivated HER signaling in this disease. The determinants of primary resistance to MAPK inhibitors vary between cancer types, due to preferential upregulation of specific RTKs, and the abundance of their respective ligands.

Keywords

Thyroid Cancer; BRAF; Vemurafenib; HER3; Neuregulin-1

INTRODUCTION

Mutations in *BRAF* are present in ~ 50% of metastatic melanomas, 35–60% of advanced thyroid cancers, and in a lower proportion of colorectal, ovarian and lung carcinomas (1–4).

[6]Corresponding author: James A Fagin, MD, Memorial Sloan-Kettering Cancer Center, 1275 York Avenue, New York, NY 10065, United States, Tel: +1 646 888 2136, faginj@mskcc.org.
[#]Equal contribution.

Conflict of interest: JAF is a consultant for Novo Nordisk and receives grant support from AstraZeneca. NR is on the Scientific Advisory Board for Astrazeneca and Chugai, is a consultant for Novartis and receives laboratory funding from Astrazeneca and Chugai.

The small molecule RAF inhibitor vemurafenib (PLX4032, RG7204) has high specificity for the BRAF oncoprotein, and is a potent inhibitor of MAPK signaling and growth of *BRAF* mutant melanoma cell lines, but not of cancer cell lines with wild-type *BRAF* (5, 6). Vemurafenib increases overall survival and progression-free survival in patients with *BRAF* mutant metastatic melanoma. Although the clinical responses are remarkable, the beneficial effects are not durable, as the median time to progression is 5.3 months (7).

Several mechanisms may account for secondary resistance to PLX4032 in melanomas: e.g. acquisition of *RAS* mutations, overexpression of PDGFRβ, expression of a drug-resistant splice variant of BRAF-V600E with enhanced dimerization properties, overexpression of MAP3K8 (COT), among others (8–11). In addition, exposure to HGF from the stromal microenvironment can promote some degree of intrinsic resistance to RAF inhibitors in melanoma cell lines (12, 13). In contrast to the high response rate seen in patients with metastatic melanomas, PLX4032 has limited efficacy as a single agent in patients with *BRAF*-mutant colorectal cancers (14). The decreased sensitivity of many colorectal cancer cell lines to growth inhibition by PLX4032 has recently been ascribed to activation of epidermal growth factor receptor (EGFR) signaling (15, 16). This was proposed to be due to feedback-induced relaxation of the activity of CDC25C, a putative EGFR phosphatase (15).

Metastatic thyroid cancers that are refractory to radioactive iodine therapy have a particularly high prevalence of *BRAF* mutations (17). The MEK inhibitor selumetinib (AZD6244, ARRY-142886) showed minimal activity in a phase 2 study of thyroid cancer (18). A trial with vemurafenib for this disease is now in progress. Here we report that the majority of *BRAF*-mutant thyroid cancer cell lines are insensitive to the growth inhibitory effects of PLX4032, and that this is largely due to a feedback-induced ligand-dependent activation of HER2/HER3 signaling. Hence, the early response of BRAF-mutant cancers to selective MAPK pathway inhibitors is marked by the relaxation of oncoprotein-driven negative feedback events, which differ between tumors of various lineages, and which predict a requirement for distinct therapeutic strategies.

RESULTS

Lineage-specific differences in effects of PLX4032 on MAPK signaling and cell growth

BRAF-mutant melanoma cell lines were uniformly sensitive to growth inhibition by PLX4032 (IC_{50} < 100 nM), whereas most thyroid (5/6) and colorectal lines (3/4) were comparatively refractory (IC_{50} > 1000 nM) (Fig. 1A). PLX4032 (2 μM) evoked a sustained inhibition in pMEK and pERK in melanoma cell lines through 72 h. By contrast, the inhibition of RAF effectors in *BRAF*-mutant thyroid and colorectal cell lines was transient, with a rebound beginning 6 h after addition of the drug in 5/6 thyroid and 3/4 colorectal cancer cell lines (Fig. 1B). The excursions in pERK were consistent with the gene expression kinetics of the ERK phosphatase DUSP5, a component of the transcriptional output driven by MAPK activation (Supplementary Fig. S1A) (19). The rebound in pERK was not due to rapid drug metabolism, as re- addition of 2 μM PLX4032 72 h after initial exposure did not re-inhibit the pathway (Fig. 1C), whereas addition of the MEK inhibitor AZD6244 had a potent effect (Supplementary Fig. S1B). The rebound in MAPK signaling seen after treatment with PLX4032 likely contributes to attenuate the biological response to RAF inhibition.

Treatment of thyroid cancer cell lines with RAF inhibitors is associated with RAS activation and increased expression and phosphorylation of RTKs

In cancer cells with mutant BRAF, signaling inputs upstream of the oncoprotein are inhibited by negative feedback (20). As shown in Fig. 1D, treatment of the thyroid cell line

SW1736 with PLX4032 led to a time-dependent increase in GTP-bound RAS, consistent with relaxation of the negative feedback upstream of RAF, which was of a much greater magnitude in thyroid as compared to the SK-Mel-28 melanoma cells. The increase in RAS activity is potentially significant, as enforced RAS activation can overcome the PLX4032-induced block of MAPK in mutant BRAF melanoma cells (8, 21). We used two different screens to identify potential mediators of these effects. We first obtained gene expression profiles at 0, 1, 6 and 48 h after addition of PLX4032 to SW1736 and SK-MEL-28 cells, and identified several gene clusters with significantly different expression kinetics between the thyroid and melanoma lines (Supplementary Fig. S2A). Functional enrichment analysis against the KEGG database revealed overrepresentation of the following terms in SW1736 compared to SK-MEL-28 cells: ErbB signaling pathway, Insulin signaling pathway, Cytokine-cytokine receptor pathway and MAPK signaling pathway (Supplementary Fig. S2B). These gene clusters include several RTKs such as *HER2*, *PDGFRβ*, *EGFR* and *EPHB2*, whose expression differences were confirmed by semiquantitative RT-PCR (Supplementary Fig. S2C).

As an additional screen for receptor tyrosine kinases (RTK) potentially activated in response to the RAF inhibitor in SW1736 cells, we incubated lysates of cells treated with or without 2 μM PLX4032 with human phospho-RTK arrays. Treatment with PLX4032 increased HER3 phosphorylation by > 11-fold, and modestly induced phosphorylation of several members of the ephrin family. There was no detectable increase in EGFR phosphorylation (Fig. 2A). Western blots showed induction of total HER2 and HER3, which was associated with a marked increase in HER3 phosphorylation at Y1197 and Y1289 after PLX4032 treatment. This in turn was associated with a rebound in pERK and transient activation of AKT (Fig. 2B). We next examined whether the changes seen in SW1736 cells were also present in other *BRAF* mutant cancer cell lines. HER3 phosphorylation was induced in 5/6 thyroid, but was low or undetectable in melanoma and colorectal lines (Fig. 2C and Supplementary Fig. S3A). Four of 6 thyroid cancer cell lines showed decreased pEGFR 72 h after vemurafenib, whereas there was no change in colorectal lines (Fig. 2C and Supplementary Fig. S3A).

HER2 and HER3 expression and activation were also markedly increased by the allosteric MEK inhibitor PD0325901 6 h post-treatment in thyroid cancers of *TPO-Cre/LSL-Braf*^{V600E} mice, a genetically accurate model of thyroid tumorigenesis induced by endogenous expression of the oncoprotein (22) (Fig. 2D).

PLX4032 induces the expression and activation of HER2/HER3 heterodimers in thyroid cancer cells

Thus, following treatment of BRAF-mutant thyroid cancer cells with vemurafenib there is a relief of feedback that results in increased expression of the RTKs HER2 and HER3 and this is associated with RAS activation. HER3 is a kinase-impaired member of the HER family, which is phosphorylated and activated by heterodimerization with one of the other family members (HER2, EGFR or HER4). To identify the HER3 dimer partner we depleted the expression of EGFR or HER2 by RNA interference in 8505C thyroid cells (Fig. 3A). PLX4032-induced HER3 phosphorylation was inhibited by knockdown of HER2 but not of EGFR. Moreover, co-immunoprecipitation of either HER3 or HER2 resulted in pulldown of the reciprocal partner, confirming the induction of HER2/HER3 complexes by 2 μM PLX4032 in both cell lines (Fig. 3B). Of the various HER dimers, the HER2/HER3 heterodimer is considered the most potent signaling unit (23). The C-terminal residues of these receptors provide docking sites for the adaptor protein GRB2 (HER2>HER3) and the p85 regulatory subunit of PI3Kinase (HER3>HER2). These molecules couple the heterodimer to the RAS/RAF/MAPK and PI3K signaling pathways, respectively (24). Immunoprecipitation of HER3 confirmed the recruitment of p85 after PLX4032 treatment (Fig. 3B). Similarly, IP of either HER3 or HER2 after PLX4032 was associated with

increased recruitment of GRB2, likely accounting for the induction of RAS signaling (Fig. 3C). Moreover, treatment of 8505C cells with the HER kinase inhibitor lapatinib abrogated the PLX4032-induced phosphorylation of HER3, recruitment of p85 to HER3, and the increase in RAS-GTP levels (Fig. 3D and 3E). Addition of lapatinib also largely prevented the activation of pAKT and pERK in SW1736 and 8505C cells exposed to the RAF inhibitor (Fig. 3F).

PLX4032-induced HER2/HER3 activation is dependent on autocrine neuregulin expression and is augmented by exogenous addition of the ligand

Neuregulin-1 (NRG1) is the major HER3 ligand, which promotes its engagement with HER2 kinase and the subsequent transphosphorylation of HER3 (25). To investigate whether PLX4032-induced activation of HER2/HER3 is mediated by NRG1, we deprived 8505C cells of serum for 24 h in the absence or presence of 2 μM PLX4032. Serum starvation did not entirely shut down the HER3 phosphorylation induced by PLX4032 (Fig. 4A, lane 5 vs 2), pointing to the existence of either a basal level of ligand-independent HER3 activation, or an autocrine production of NRG1. Knock-down of NRG1 markedly inhibited HER3 phosphorylation in cells incubated in serum-free medium, consistent with autocrine secretion of the ligand (Fig. 4B). Addition of exogenous NRG1 further stimulated HER3 phosphorylation, even in the absence of PLX4032 (Fig. 4A, lanes 3 versus 4), suggesting that basal co-expression of HER3 and HER2, although low, was sufficient to be efficiently activated by NRG1, and to transduce signaling via AKT and ERK effectors. Addition of NRG1 to PLX4032 pretreated cells superactivated HER3, PI3K and MAPK signaling (lane 6) and this was blocked by 1 μM lapatinib (lane 7). The HER2 antagonist pertuzumab also inhibited signaling in thyroid cancer cell lines exposed to endogenous NRG1 (Fig. 4C). Interestingly, expression of NRG1 was consistently higher in *BRAF*-mutant thyroid than in melanoma or colorectal cell lines (Fig. 4D and E). Some melanoma cell lines, such as SK-MEL-28, do show some increase in total HER3 after exposure to PLX4032 (Supplementary Fig. S4A), but no HER3 phosphorylation because they do not secrete NRG1. Treatment of SK-MEL-28 cells with exogenous ligand induced HER2/HER3 signaling (Supplementary Fig. S4B) and attenuated the growth-inhibitory effects of PLX4032 (Supplementary Fig. S4C).

Inhibition of oncogenic BRAF increases HER3 gene transcription

We next examined the mechanisms accounting for the increase in HER3 by MAPK pathway inhibitors in *BRAF* mutant thyroid cell lines. Upregulation of HER3 has been found to mediate resistance to PI3K/AKT (26) or HER2 (27) inhibitors in HER2-amplified breast cancer cell lines, which is caused in part through a FoxO3A-dependent induction of HER3 gene transcription. As shown in Fig. 5A, PLX4032 treatment increased HER3 and HER2 mRNAs in all six BRAF-mutant thyroid cancer cell lines tested. Similar results were found following treatment with the MEK inhibitor AZD6244 (not shown). The effects of the MEK inhibitor on total HER2, HER3 protein and on pHER3 were dose dependent, and inversely associated with the degree of inhibition of pERK (Fig. 5B). RAF or MEK inhibitors induced luciferase activity of a HER3 promoter construct spanning ~ 1 kb upstream of the transcriptional start site in 8505C cells. Serial deletions identified a minimal HER3 promoter retaining transcriptional response to vemurafenib and AZD6244, which was located between −401 and −42 bp (Fig. 5C). This region does not contain any predicted FoxO binding sites. Moreover, PLX4032 led to an increase in phosphorylation of FoxO1/3A between 4–10h after addition of compound (not shown), which is known to promote its dissociation from DNA, and likely discards involvement of these factors as transcriptional regulators of HER3 in response to MAPK pathway inhibition. The minimal HER3 promoter region regulated by MAPK inhibitors overlaps with sequences previously described to be immunoprecipitated using antibodies against the ZFN217 transcription factor and CtBP1/CtBP2 corepressors

(28–30). CtBPs have also been described to negatively regulate transcriptional activity of the HER3 promoter in breast carcinoma cell lines (30). Silencing of CtBP1, and to a lesser extent CtBP2, increased basal HER3 in 8505C cells, and markedly potentiated the effects of PLX4032 (Fig. 5D and 5E). Knockdown of these factors modestly increased basal and PLX4032-induced HER2 levels, which likely contributes to the remarkable increase in pHER3 we observed (Fig. 5D and 5E). Finally, CtBP1 and CtBP2 chromatin immunoprecipitation assays showed decreased binding to the HER3 promoter after treatment with PLX4032 (Fig. 5F). These findings were confirmed in a second cell line (Supplementary Fig. S5A).

The HER kinase inhibitor lapatinib cooperates with RAF or MEK inhibitors to inhibit thyroid cancer cell growth *in vitro*

To examine if HER2/HER3 activation mediates resistance to PLX4032, we treated SW1736, 8505C and Hth104 for 4 days with increasing concentrations of the RAF inhibitor with or without 1 μM lapatinib, or with 2 μM PLX4032 combined with increasing doses of lapatinib. As shown in Fig. 6A, lapatinib alone markedly sensitized the three cell lines to dose-dependent inhibition by the RAF inhibitor. The IC_{50} for PLX4032 shifted from ≥ 1.5 μM in the three cell lines to 0.19, 0.97 and 0.49 μM, respectively. Accordingly, the fraction of cells in G1 was significantly higher when 2 μM PLX4032 was combined with 1 μM lapatinib (Fig. 6B). The percent of cells in sub-G1 was greater in cells treated with the combination, however at levels that are not likely to be biologically significant (not shown). Knock-down of HER3 by shRNA also increased the sensitivity to PLX4032 in SW1736 cells (Supplementary Fig. S6A). Treatment of SW1736 cells with the MEK inhibitor AZD6244 also results in robust activation of HER3 signaling (Supplementary Fig. S6B). Accordingly, lapatinib shifted the IC_{50} for the MEK inhibitor (34 to 18 nM, and 330 to 110 nM in SW1736 and 8505C cells, respectively) (Supplementary Fig. S6C), and significantly increased the fraction of cells in G1 (Fig. 6B). We next tested the effects of lapatinib, the RAF inhibitor PLX4720 or their combination in thyroid cancers of *TPO-Cre/LSL-Braf*^{V600E} mice (22). The combination resulted in a greater inhibition of mitotic rate than PLX4720 alone and in a significant reduction of thyroid volume (Fig. 6C and 6D).

Role of other RTKs in the intrinsic resistance of thyroid cancers to RAF inhibitors

Expression profiling (Supplementary Fig. S2C) and the RTK phosphoarray (Fig. 2A) show that in addition to HER3 there was upregulation of expression and/or phosphorylation of Ephrins and of PDGFRβ in response to vemurafenib. This is of interest because activation of PDGFRβ has been proposed as a mechanism of acquired resistance to PLX4032 in patients with metastatic melanoma (8). Western blots showed a marked induction of PDGFRβ in SW1736 cells by the RAF inhibitor. PDGFRβ was induced to a much lesser extent in RKO-1 and T235 cells, and was constitutively high in Hth104 cells (Supplementary Fig. S7A). Despite the remarkable increase in PDGFRβ in SW1736 cells after PLX4032 treatment, stimulation with PDGF-BB only activated pAKT and pERK modestly at a time when the receptor was maximally expressed (Supplementary Fig. S7B). By contrast, stimulation with NRG1 under the same conditions induced a far greater activation of signaling, indicating that the HER2/HER3 dimer is dominant under these conditions. Moreover, treatment with the PDGFR inhibitor imatinib failed to sensitize SW1736 cells to growth suppression by PLX4032 (Supplementary Fig. S7C).

As EGFR has been implicated in resistance to vemurafenib in colorectal cancer and melanoma cell lines (16, 31, 32), we further investigated the possible contribution of this receptor to the insensitivity to RAF inhibition in thyroid cancer cells. Of note, pEGFR decreased 24 and 48 h after vemurafenib, corresponding to the peak of pHER3 and pERK (Fig. 3F). Knockdown of EGFR did not sensitize 8505C cells to PLX4032 (Supplementary

Fig. S7D), and indeed paradoxically decreased sensitivity to the compound. By contrast, knockdown of HER2 significantly augmented the growth inhibitory effects of vemurafenib (Supplementary Fig. S7D). Treatment with cetuximab also failed to sensitize in 8505C and Hth104 cells to RAF kinase inhibition (not shown).

DISCUSSION

Oncogenic drivers reprogram the signaling network of cancer cells, in part by inducing negative feedback events (33). Targeted therapies may relieve those feedbacks and reengage pathways that limit the antitumor response. What is underappreciated, and is demonstrated in this report, is that the receptors that are reactivated are to a significant extent lineage specific and dependent on the availability of their cognate ligands. Moreover, not all reactivated pathways drive resistance to therapy, emphasizing the need to explore their functional consequences in detail. The corollary to this is that tumors of different cell types harboring the same activated oncoprotein respond in a different way to selective inhibitors, through mechanisms that are tractable and that may in part be anticipated based on the cell of origin.

Activation of MAPK signaling in normal cells occurs in response to growth factors, cytokines and stress signals. BRAF transformed cells hyperactivate MAPK independently of upstream inputs, to which cells become unresponsive through induction of ERK-dependent negative feedback loops (33). Accordingly, RAS-GTP levels are depleted in *BRAF*-mutant tumor cells regardless of their cell type and, as shown in this paper, the activation state of RTKs is low. When exposed to RAF or MEK inhibitors BRAF-mutant melanoma and thyroid cells show markedly different MAPK signaling kinetics. Whereas thyroid cancer cells are primed to reactivate the pathway shortly after exposure to the kinase inhibitors, melanoma cells are not. Thyroid cells show rapid increases in RAS-GTP in response to RAF kinase inhibition, consistent with the activation of upstream signals. The MAPK rebound was not affected by re-addition of PLX4032, likely because of its relative selectivity for monomeric mutant BRAF (21). By contrast, the MEK inhibitor AZD6244 suppressed the RAF inhibitor-induced ERK rebound, presumably by interrupting upstream signals mediated by wild-type RAF proteins. There was a more pronounced rebound in ERK compared to MEK phosphorylation after vemurafenib, which may be due to transient downregulation of ERK phosphatases (e.g. DUSP5), in particular at early time points after exposure to the drug.

Two different screening approaches pointed to an increase in the expression and activation of RTKs as primary candidates in mediating the rebound in MAPK activity after treatment with RAF or MEK inhibitors. We focused on HER3 because it showed the greatest magnitude change in phosphorylation in the index line, and because its activation was the most prevalent across all other thyroid lines we tested. Indeed, both HER3 and HER2 mRNA levels increased ubiquitously in thyroid cancer cells treated with vemurafenib. HER3 is a kinase inactive receptor that requires heterodimerization to transduce signaling. Co-immunoprecipitation assays and transient knockdown of possible dimer partners led us to identify HER2 as the principal HER3 partner. We did not detect any significant increase in EGFR phosphorylation in response to vemurafenib in any of the thyroid cell lines we tested. EGFR activation has been recently linked to unresponsiveness to MAPK inhibition in BRAF mutant melanoma and colorectal cancer cells (32, 31). In the latter study, the authors also proposed that the same mechanism likely accounted for the unresponsiveness of thyroid cancer cell lines to RAF inhibitors. This conclusion was based in part on the demonstration that gefitinib enhanced the growth inhibitory effects of PLX4032 in 8505C and BHT101 thyroid cancer cells; however the EGFR-specific monoclonal antibody cetuximab had no effect. In our hands cetuximab or EGFR knockdown also failed to sensitize thyroid cancer

cells to vemurafenib, whereas HER3 or HER2 knockdown had significant growth inhibitory effects. However, HER3 interactions with other ERB family kinases can be promiscuous, suggesting that co-targeting of HER2 and EGFR with kinase inhibitors may be a productive approach to sensitize cells to MAPK pathway inhibition.

HER2/HER3 signaling is controlled by HER2-overexpression or ligand binding. As HER2 has no known ligand, the heterodimer is primarily induced by the HER3 ligand NRG1 (24), which can be produced by tumor cells or by tumor stroma. The importance of tumor production of NRG-1 was recently demonstrated in non-*HER2* amplified cancer cells, which were found to be dependent on a NRG1-mediated autocrine loop (34, 35). These cell lines, mainly from head and neck tumors, showed HER3 expression and phosphorylation and sensitivity to lapatinib (35). All thyroid cancer cell lines we tested expressed NRG-1, and knockdown of NRG-1 markedly inhibited HER3 phosphorylation, suggesting that the HER3 activation by MAPK pathway blockade is dependent on this autocrine loop. Interestingly, 2 of the 4 melanoma cell lines we tested showed an induction of HER3 expression by PLX4032 treatment, but no evident HER3 activation. By contrast to thyroid cells, basal expression of NRG-1 was not detectable in melanoma cells. When ligand was added to their media, HER2/HER3 signaling was activated, leading to an attenuation of the growth inhibitory effects of PLX4032. Colorectal cancer cell lines express low levels of HER3 constitutively, but no NRG1, and hence HER3 activation does not ensue. Hence, the peculiar resistance to RAF and MEK inhibitors of *BRAF* mutant thyroid cancers is due to a combination of factors: i.e. the induction of HER3 expression by MAPK inhibitors, and the constitutive autocrine production of its ligand (Figure 7).

The increase in expression of HER3 after MAPK inhibition is due to activation of gene transcription, which was associated with a reduction of binding of the transcriptional repressors CTBP1 and CTBP2 to the *HER3* gene promoter. These corepressors have been previously linked to inhibition of HER3 transcription through promoter regions that show overlapping occupancy with ZNF217, a transcription factor also involved in HER3 regulation (30). Accordingly, knockdown of CTBPs acutely induced HER3 expression and phosphorylation in thyroid cancer cells. MAPK inhibition may dictate a chromatin redistribution of these repressors, and thus activate HER3 transcription. The biochemical mechanisms involved in delocalization of CtBPs by MAPK inhibition have not been explored, but posttranslational modifications are known to regulate the repressive activity of CtBPs either by translocation to the cytoplasm or by targeting them for degradation (36, 37).

Besides the activation of HER3, there was either induction or high basal levels of expression of other RTKs in thyroid cancer cell lines exposed to MAPK pathway inhibitors, such as PDGFRβ, previously implicated in acquired resistance to vemurafenib in patients with metastatic melanoma (8). However, treatment with the PDGFR kinase inhibitor imatinib did not sensitize the cancer cells to the growth inhibitory effects of the RAF inhibitor. These findings have potentially significant clinical ramifications. A commonly advocated approach to identify mechanisms of intrinsic or acquired resistance to kinase inhibitors such as vemurafenib in clinical trials is to biopsy tumor sites while patients are on therapy to assay for expression and phosphorylation of RTKs or other signaling proteins. The findings described here show that this could be misleading, as simple demonstration of RTK overexpression or phosphorylation is not likely to point to the functionally relevant signaling unit. Instead, a deeper understanding of lineage-specific determinants of response to MAPK inhibition is more likely to be rewarding, and guide selection of appropriate combination therapies.

MATERIAL AND METHODS

Reagents

PLX4032 and PLX4720 were from Plexxikon and AZD6244 was from AstraZeneca. Lapatinib and imatinib were purchased from Selleck Chemicals. All drugs were dissolved in DMSO for *in vitro* studies. For *in vivo* studies, PD0352901 and lapatinib were dissolved in 0.5% hydroxylpropylmethylcellulose/0.2% Tween 80 (Sigma) and 0.5% hydroxypropylmethylcellulose/0.1% Tween-80 (Sigma), respectively, and administered by oral gavage. Recombinant human NRG-1 (#5218SC) and hPDGFBB (#8912SC) were from Cell Signaling Technology. A detailed list of antibodies and sources is included in Supplemental Experimental Procedures.

Cell culture

Cancer cell lines were maintained at 37°C and 5% CO_2 in humidified atmosphere and grown in RPMI 1640 or DMEM growth media supplemented with 10% of fetal bovine serum, 2mM glutamine, 50 U/ml penicillin (GIBCO) and 50 μg/ml streptomycin. BHT101 cells were grown in MEM supplemented with 20% of fetal bovine serum. Melanoma and colorectal cancer cell lines were a gift from D. B. Solit (MSKCC, NY). All thyroid cancer cell lines used in this study were authenticated using short tandem repeat and single nucleotide polymorphism array analysis (38). For cell growth assays, cells were plated in triplicate into 6-well plates at 5×10^4 cells/well, and treated with DMSO or increasing concentrations of the indicated drug for 4 days. Cells were collected by trypsinization and counted in a Vi-Cell series cell viability analyzer (Beckman Coulter). IC_{50} values were calculated by nonlinear regression using Prism v5.04 (GraphPad Software).

Cell cycle analyses

Cells were plated in triplicate into 60-mm dishes at a density of $1–2.5 \times 10^5$ cells/well. Next day cells were treated with DMSO or the indicated drug. After 48 h adherent and floating cells were harvested and stained with ethidium bromide (39). Flow cytometric analysis was used for quantification of cell-cycle distribution.

Immunoblotting

Cells were harvested by trypsinization, washed twice with cold PBS, and lysed in NP-40 buffer (containing 25 ml of 1 M Tris pH 7.4, 15 ml of 5 M NaCl, 20 ml of 1 M NaF, 5 ml of NP-40 and 435 ml of distilled water). Protein concentration was determined using the BCA kit (Thermo Scientific). Western blots were performed on 25 μg protein separated by SDS-7.5–10% PAGE using the indicated antibodies. For immunoprecipitation assays, a volume of 500 μl of lysis buffer containing equal amount of proteins was incubated with indicated antibody overnight at 4 °C with gentle rotation. Protein G magnetic beads (Invitrogen) were added for 2 h and washed three times with lysis buffer before suspension in SDS-loading buffer. RAS-GTP immuprecipitation was performed using RAS activation assay kit from Millipore according to the manufacturer's protocol. For detection of secreted NRG1, cell media was concentrated using 3K Millipore Amicon Ultra (3K) centrifugal filters at 4000 g for 40 min (35).

RNA interference

Cells were plated at 20% of confluence in medium without antibiotics and transfected with 5 nM siRNA and Lipofectamine™ RNAiMAX Transfection Reagent (Invitrogen) as indicated in the manufacturer's protocol. SiRNAs for EGFR (#s565), HER2 (#s611), HER3 (#s4779 and #s4780), NRG1 (#s194522), CtBP1 (#s3699), CtBP2 (#s3702) and negative control (#AM4611) were purchased from Ambion.

Phospho-RTK arrays

Human Phospho-RTK arrays were used according to the manufacturer's instructions (R & D Systems). Briefly, cells were washed with cold PBS and lysed in NP40 lysis buffer with 10% glycerol, and 100 μg of lysates was incubated with blocked membranes overnight. Membranes were then washed and exposed to chemiluminescent reagent and then to X-ray film. Quantification of pixels was performed by densitometry using Kodak MI software.

Semi-quantitative PCR

Total RNA was extracted using TRIZOL® Reagent (Invitrogen) and subjected to DNase I Amplification Grade (Invitrogen). For quantitative RT-PCR, mRNA was retrotranscribed using SuperScript® III First-Strand Synthesis Super Mix (Invitrogen). Real-time PCR was performed using standard conditions and Power SYBR® Green PCR master mix (Applied Biosystems) with AB-7500 System and analyzed with Q-Gene Core Module file (40). Primer sequences are shown in the Supplemental Experimental Procedures.

Cloning of *HER3* promoter constructs and luciferase assays

PCR-amplified fragments of the human *HER3* promoter (−992/+63, −730/+63, −401/−63 and −42/+63, relative to transcription start site) were cloned using BglII and KpnI restriction sites of pGl3b reporter plasmid (BglII-*HER3*-992: 5′-CGGGGTACCTAGCAGGGCTTTGGGCAGCAA-3′; BglII-*HER3*-730: 5′-CGGGGTACCCCAGACTCCAGTGTGGAAGG-3′; BglII-HER3–401: 5′-CGGGGTACCCTCCCCCTCAAAAACACAC-3′; BglII-*HER3*-42: 5′-CGGGGTACCCCTTCCCTCTGCGTTCCT-3′ and KpnI-*HER3*+63: 5′-GGAAGATCTAAATTGCAATCGGAGCCGGAGC-3′). 8505C cells were transiently transfected using Lipofectamine 2000 (Invitrogen), 1 μg of reporter construct and 60 ng of pRL-CMV. Twelve hours post-transfection, 2 μM vemurafenib or 0.5 μM AZD6244 were added to 8505C in complete media and cells harvested at the indicated time points, lysed, and analyzed for luciferase and renilla activities. The promoter activity was determined as the ratio between luciferase and renilla, relative to the ratio obtained in non-treated cells. The results shown are the mean ± SD of two independent experiments, each performed in triplicate.

Chromatin immunoprecipitation

ChIP samples were prepared from 8505C cells as follows: cultures of 25×10^6 cells were treated with or without 2 μM PLX4032 during 24 h. Then, cross-linking was performed with 1% formaldehyde for 10 min at room temperature. Cross-linking was stopped by the addition of glycine to a final concentration of 125 mM, and cells were washed twice with PBS. The cell pellet was resuspended consecutively in ChIP lysis buffers (41) and sonicated using the Bioruptor sonicator (Diagenode) to produce chromatin fragments of 200–500 bp on average. Sheared chromatin was incubated with CtBP1 (BD Biosciences, #612042) or CtBP2 (BD Biosciences, #612044) mouse antibody-coated magnetic beads. To prepare the coated beads, 75 μl Dynabeads Protein G (Invitrogen) were incubated overnight with 7.5 μg of the above mentioned antibodies. The following day, the beads were rinsed and added to the sheared chromatin and incubated overnight at 4 °C. Samples were then rinsed eight times with RIPA buffer, and the antibody stripped from the beads by incubating in 1% SDS at 65 °C for 15 min; cross-linking was reversed by incubating overnight at 65 °C. The next day, samples were sequentially treated with RNAse A and Proteinase K, and DNA was extracted using Qiaquick PCR Purification kit (Qiagen Sciences). Controls included an input condition obtained before DNA-protein immunoprecipitation. Semi-quantitative PCR reactions to confirm enrichment of HER3 promoter sequences were performed as described. ChIP ratio was calculated as enrichment over noise normalized to the input.

Animal Studies

Three week-old *LSL-Braf/TPO-Cre* mice were treated with a single dose of PD0352901 (25 mg/kg). Thyroids were collected before and 6 h after administering PD352901 and snap frozen in liquid N2. Proteins were extracted and Western blots performed as described. To test the effects of PLX4720 alone or in combination with lapatinib on tumor growth, 4–6 week-old *LSL-Braf/TPO-Cre* mice were treated for 3 weeks with lapatinib (150 mg/kg five times a week), PLX4720-impregnated chow, or their combination. Thyroid imaging was performed at day 0 and day 21 with a Vevo 2100 micro-ultrasound system and volumes calculated with the Vevo 2100 imaging software version 1.3.0. To determine effects on mitotic rate, mice were treated for 2 weeks as above except that lapatinib was administered three times a week. Thyroids were collected 6 hours after the final dose of lapatinib, fixed in 4% para-formaldehyde and representative sections stained with Ki67 antibody (Vector Laboratories; 0.05 μg/mL). All procedures were conducted in accordance with the Guidelines for the Care and Use of Laboratory Animals and were approved by the Institutional Animal Care and Use Committees (IACUCs) at Memorial Sloan-Kettering Cancer Center.

Statistical analysis

Statistical significance of differences between the results was assessed using a standard two-tailed t test and Mann-Whitney test for in vivo data, performed using Prism v5.04 (GraphPad Software). $p < 0.05$ was considered statistically significant.

Data deposition

The microarray data reported in this paper have been deposited in NCBI's Gene Expression Omnibus (GEO) database, www.ncbi.nlm.nih.gov/geo (accession no. GSE37441).

Supplementary Material

Refer to Web version on PubMed Central for supplementary material.

Acknowledgments

Financial support: This work was supported by grants from the National Institutes of Health (CA50706 and CA72598, to J.A.F). C.M-C. and S. R-L. were partially supported by Spanish Ministry of Science and Innovation (BMED 2008-0659 and BMED 2009-0187, respectively). J.M.D. was partially supported by Pontificia Universidad Catolica and Becas Chile (#76100021). We also thank the Hearst Family, Lefkofsky, Byrne and Margot Rosenberg Pulitzer Foundations and the Society of MSKCC for their generous support.

We thank I. Vivanco for the retroviral HER3 shRNA construct. We thank G. Bollag at Plexxikon Inc. for providing PLX4032 and PLX4720, P. Chi for advice on ChiP experiments and C. L. Sawyers for helpful comments on the manuscript. We thank the MSKCC Genomic Core Facility for the expression profiling experiments.

Reference List

1. Davies H, Bignell GR, Cox C, Stephens P, Edkins S, Clegg S, et al. Mutations of the BRAF gene in human cancer. Nature. 2002; 417:949–54. [PubMed: 12068308]
2. Kimura ET, Nikiforova MN, Zhu Z, Knauf JA, Nikiforov YE, Fagin JA. High prevalence of BRAF mutations in thyroid cancer: genetic evidence for constitutive activation of the RET/PTC-RAS-BRAF signaling pathway in papillary thyroid carcinoma. Cancer Res. 2003; 63:1454–7. [PubMed: 12670889]
3. Xing M. BRAF mutation in papillary thyroid cancer: pathogenic role, molecular bases, and clinical implications. Endocr Rev. 2007; 28:742–62. [PubMed: 17940185]

4. Paik PK, Arcila ME, Fara M, Sima CS, Miller VA, Kris MG, et al. Clinical characteristics of patients with lung adenocarcinomas harboring BRAF mutations. J Clin Oncol. 2011; 29:2046–51. [PubMed: 21483012]
5. Yang H, Higgins B, Kolinsky K, Packman K, Go Z, Iyer R, et al. RG7204 (PLX4032), a selective BRAFV600E inhibitor, displays potent antitumor activity in preclinical melanoma models. Cancer Res. 2010; 70:5518–27. [PubMed: 20551065]
6. Joseph EW, Pratilas CA, Poulikakos PI, Tadi M, Wang W, Taylor BS, et al. The RAF inhibitor PLX4032 inhibits ERK signaling and tumor cell proliferation in a V600E BRAF-selective manner. Proc Natl Acad Sci U S A. 2010; 107:14903–8. [PubMed: 20668238]
7. Chapman PB, Hauschild A, Robert C, Haanen JB, Ascierto P, Larkin J, et al. Improved survival with vemurafenib in melanoma with BRAF V600E mutation. N Engl J Med. 2011; 364:2507–16. [PubMed: 21639808]
8. Nazarian R, Shi H, Wang Q, Kong X, Koya RC, Lee H, et al. Melanomas acquire resistance to B-RAF(V600E) inhibition by RTK or N-RAS upregulation. Nature. 2010; 468:973–7. [PubMed: 21107323]
9. Johannessen CM, Boehm JS, Kim SY, Thomas SR, Wardwell L, Johnson LA, et al. COT drives resistance to RAF inhibition through MAP kinase pathway reactivation. Nature. 2010; 468:968–72. [PubMed: 21107320]
10. Villanueva J, Vultur A, Lee JT, Somasundaram R, Fukunaga-Kalabis M, Cipolla AK, et al. Acquired resistance to BRAF inhibitors mediated by a RAF kinase switch in melanoma can be overcome by cotargeting MEK and IGF-1R/PI3K. Cancer Cell. 2010; 18:683–95. [PubMed: 21156289]
11. Poulikakos PI, Persaud Y, Janakiraman M, Kong X, Ng C, Moriceau G, et al. RAF inhibitor resistance is mediated by dimerization of aberrantly spliced BRAF(V600E). Nature. 2011; 480:387–90. [PubMed: 22113612]
12. Straussman R, Morikawa T, Shee K, Barzily-Rokni M, Qian ZR, Du J, et al. Tumour micro-environment elicits innate resistance to RAF inhibitors through HGF secretion. Nature. 2012; 487:500–4. [PubMed: 22763439]
13. Wilson TR, Fridlyand J, Yan Y, Penuel E, Burton L, Chan E, et al. Widespread potential for growth-factor-driven resistance to anticancer kinase inhibitors. Nature. 2012; 487:505–9. [PubMed: 22763448]
14. Kopetz S, Desai J, Chan E, Hecht JR, O'dwyer PJ, Lee RJ, et al. PLX4032 in metastatic colorectal cancer patients with BRAF tumors. J Clin Oncol. 2010; 28:7s. Ref Type: Abstract.
15. Prahallad A, Sun C, Huang S, Di NF, Salazar R, Zecchin D, et al. Unresponsiveness of colon cancer to BRAF(V600E) inhibition through feedback activation of EGFR. Nature. 2012:10. [PubMed: 22222729]
16. Corcoran RB, Ebi H, Turke AB, Coffee EM, Nishino M, Cogdill AP, et al. EGFR-mediated reactivation of MAPK signaling contributes to insensitivity of BRAF mutant colorectal cancers to RAF inhibition with vemurafenib. Cancer Discov. 2012; 2:227–35. [PubMed: 22448344]
17. Ricarte-Filho JC, Ryder M, Chitale DA, Rivera M, Heguy A, Ladanyi M, et al. Mutational profile of advanced primary and metastatic radioactive iodine-refractory thyroid cancers reveals distinct pathogenetic roles for BRAF, PIK3CA, and AKT1. Cancer Res. 2009; 69:4885–93. [PubMed: 19487299]
18. Hayes DN, Lucas AS, Tanvetyanon T, Krzyzanowska MK, Chung CH, Murphy B, et al. Phase II efficacy and pharmacogenomic study of selumetinib (AZD6244; ARRY-142886) in iodine-131 refractory papillary thyroid carcinoma (IRPTC) with or without follicular elements. Clin Cancer Res. 2012
19. Pratilas CA, Taylor BS, Ye Q, Viale A, Sander C, Solit DB, et al. (V600E)BRAF is associated with disabled feedback inhibition of RAF-MEK signaling and elevated transcriptional output of the pathway. Proc Natl Acad Sci U S A. 2009; 106:4519–24. [PubMed: 19251651]
20. Lito P, Pratilas CA, Joseph EW, Tadi M, Zubrowski M, Huang A, et al. Relief of profound inhibition of mitogenic signaling by Raf inhibitors attenuates their activity in BRAFV600E melanomas. Cancer Cell. 2012; 22:668–82. [PubMed: 23153539]

21. Poulikakos PI, Zhang C, Bollag G, Shokat KM, Rosen N. RAF inhibitors transactivate RAF dimers and ERK signalling in cells with wild-type BRAF. Nature. 2010; 464:427–30. [PubMed: 20179705]
22. Franco AT, Malaguarnera R, Refetoff S, Liao XH, Lundsmith E, Kimura S, et al. Thyrotrophin receptor signaling dependence of Braf-induced thyroid tumor initiation in mice. Proc Natl Acad Sci U S A. 2011; 108:1615–20. [PubMed: 21220306]
23. Tzahar E, Waterman H, Chen X, Levkowitz G, Karunagaran D, Lavi S, et al. A hierarchical network of interreceptor interactions determines signal transduction by Neu differentiation factor/neuregulin and epidermal growth factor. Mol Cell Biol. 1996; 16:5276–87. [PubMed: 8816440]
24. Olayioye MA, Neve RM, Lane HA, Hynes NE. The ErbB signaling network: receptor heterodimerization in development and cancer. EMBO J. 2000; 19:3159–67. [PubMed: 10880430]
25. Wallasch C, Weiss FU, Niederfellner G, Jallal B, Issing W, Ullrich A. Heregulin-dependent regulation of HER2/neu oncogenic signaling by heterodimerization with HER3. EMBO J. 1995; 14:4267–75. [PubMed: 7556068]
26. Chandarlapaty S, Sawai A, Scaltriti M, Rodrik-Outmezguine V, Grbovic-Huezo O, Serra V, et al. AKT inhibition relieves feedback suppression of receptor tyrosine kinase expression and activity. Cancer Cell. 2011; 19:58–71. [PubMed: 21215704]
27. Garrett JT, Olivares MG, Rinehart C, Granja-Ingram ND, Sanchez V, Chakrabarty A, et al. Transcriptional and posttranslational up-regulation of HER3 (ErbB3) compensates for inhibition of the HER2 tyrosine kinase. Proc Natl Acad Sci U S A. 2011; 108:5021–6. [PubMed: 21385943]
28. Cowger JJ, Zhao Q, Isovic M, Torchia J. Biochemical characterization of the zinc-finger protein 217 transcriptional repressor complex: identification of a ZNF217 consensus recognition sequence. Oncogene. 2007; 26:3378–86. [PubMed: 17130829]
29. Krig SR, Jin VX, Bieda MC, O'Geen H, Yaswen P, Green R, et al. Identification of genes directly regulated by the oncogene ZNF217 using chromatin immunoprecipitation (ChIP)-chip assays. J Biol Chem. 2007; 282:9703–12. [PubMed: 17259635]
30. Krig SR, Miller JK, Frietze S, Beckett LA, Neve RM, Farnham PJ, et al. ZNF217, a candidate breast cancer oncogene amplified at 20q13, regulates expression of the ErbB3 receptor tyrosine kinase in breast cancer cells. Oncogene. 2010; 29:5500–10. [PubMed: 20661224]
31. Prahallad A, Sun C, Huang S, Di NF, Salazar R, Zecchin D, et al. Unresponsiveness of colon cancer to BRAF(V600E) inhibition through feedback activation of EGFR. Nature. 2012; 483:100–3. [PubMed: 22281684]
32. Girotti MR, Pedersen M, Sanchez-Laorden B, Viros A, Turajlic S, Niculescu-Duvaz D, et al. Inhibiting EGF receptor or SRC family kinase signaling overcomes BRAF inhibitor resistance in melanoma. Cancer Discov. 2012
33. Sturm OE, Orton R, Grindlay J, Birtwistle M, Vyshemirsky V, Gilbert D, et al. The mammalian MAPK/ERK pathway exhibits properties of a negative feedback amplifier. Sci Signal. 2010; 3:ra90. [PubMed: 21177493]
34. Sheng Q, Liu X, Fleming E, Yuan K, Piao H, Chen J, et al. An activated ErbB3/NRG1 autocrine loop supports in vivo proliferation in ovarian cancer cells. Cancer Cell. 2010; 17:298–310. [PubMed: 20227043]
35. Wilson TR, Lee DY, Berry L, Shames DS, Settleman J. Neuregulin-1-mediated autocrine signaling underlies sensitivity to HER2 kinase inhibitors in a subset of human cancers. Cancer Cell. 2011; 20:158–72. [PubMed: 21840482]
36. Kuppuswamy M, Vijayalingam S, Zhao LJ, Zhou Y, Subramanian T, Ryerse J, et al. Role of the PLDLS-binding cleft region of CtBP1 in recruitment of core and auxiliary components of the corepressor complex. Mol Cell Biol. 2008; 28:269–81. [PubMed: 17967884]
37. Barnes CJ, Vadlamudi RK, Mishra SK, Jacobson RH, Li F, Kumar R. Functional inactivation of a transcriptional corepressor by a signaling kinase. Nat Struct Biol. 2003; 10:622–8. [PubMed: 12872159]
38. Schweppe RE, Klopper JP, Korch C, Pugazhenthi U, Benezra M, Knauf JA, et al. Deoxyribonucleic acid profiling analysis of 40 human thyroid cancer cell lines reveals cross-contamination resulting in cell line redundancy and misidentification. J Clin Endocrinol Metab. 2008; 93:4331–41. [PubMed: 18713817]

39. Nusse M, Marx K. Flow cytometric analysis of micronuclei in cell cultures and human lymphocytes: advantages and disadvantages. Mutat Res. 1997; 392:109–15. [PubMed: 9269335]

40. Muller PY, Janovjak H, Miserez AR, Dobbie Z. Processing of gene expression data generated by quantitative real-time RT-PCR. Biotechniques. 2002; 32:1372–9. [PubMed: 12074169]

41. Lee TI, Johnstone SE, Young RA. Chromatin immunoprecipitation and microarray-based analysis of protein location. Nat Protoc. 2006; 1:729–48. [PubMed: 17406303]

SIGNIFICANCE

Thyroid cancer cell lines with mutant *BRAF* are resistant to vemurafenib. RAF inhibitors transiently inhibit the ERK pathway and de-repress HER3 transcription. In the context of constitutive NRG-1 secretion, this results in an ERK and AKT rebound that diminishes the antitumor effects of RAF inhibitors, which is overcome by combination with lapatinib.

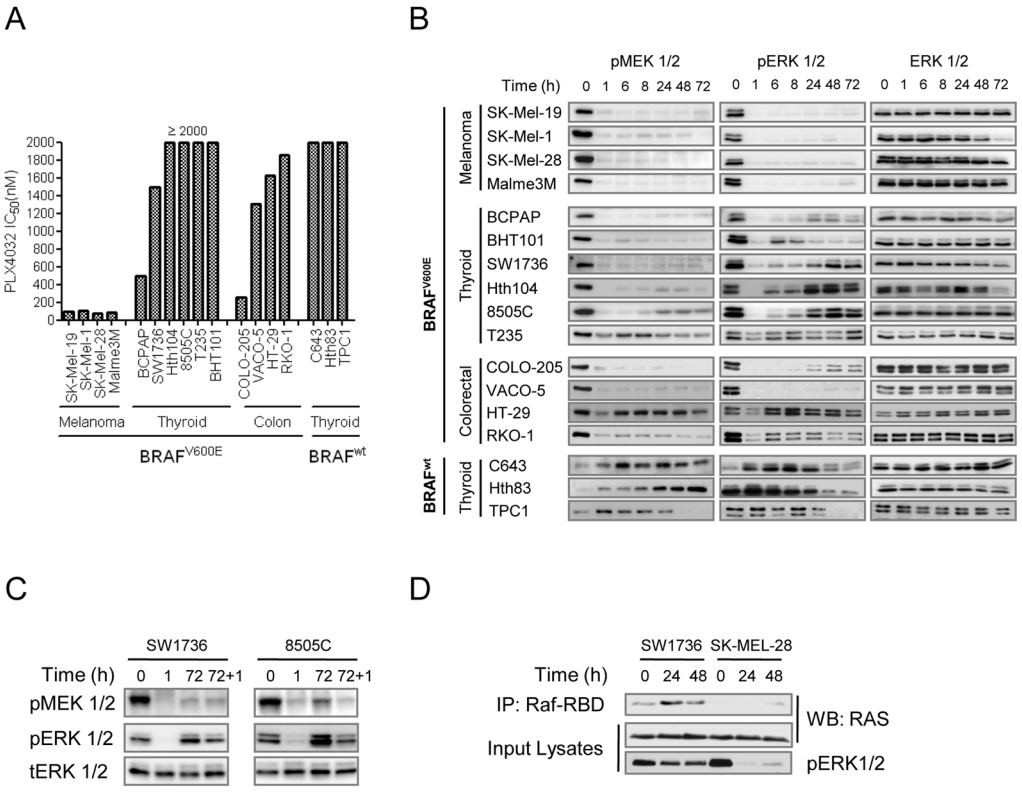

Figure 1.

Differential effects of the RAF inhibitor PLX4032 in BRAF mutant melanoma, thyroid and colorectal cancer cell lines. **A,** bars represent IC_{50} values for PLX4032 in 15 BRAF (+) cell lines. The majority of thyroid and colorectal cell lines were comparatively refractory to PLX4032, whereas melanoma lines were uniformly sensitive. A set of BRAF wild type thyroid cancer cell lines were resistant to growth inhibition by the compound. **B,** western blots of cell lines from (A) treated with 2 μM PLX4032 immunoblotted for pMEK1/2 (Ser217/221) and pERK1/2 (Thr202/Tyr204). Melanoma cell lines had a sustained inhibition of pERK1/2 after exposure to the compound, whereas most thyroid and colorectal cancer cell lines had a rebound of pERK1/2 as early as 6 h post-treatment. As expected, BRAF wild type thyroid cancer cell lines were resistant to MAPK pathway inhibition by PLX4032. **C,** SW1736 and 8505C were treated as in (B) and collected at the indicated times. 72 h post-treatment cells were re-treated with fresh PLX4032 for 1 h (lane 72 + 1). Immunoblots of pMEK1/2 and pERK1/2 demonstrated that re-addition of PLX4032 did not fully re-inhibit MAPK signaling. **D,** SW1736 and SK-MEL-28 cells were treated as in (B) and collected at 0, 24 and 48 h post-treatment. Lysates were immunoprecipitated with the RAS binding domain of CRAF (RBD) and immunoblotted for pan-RAS. Activation of RAS increased at 24 and 48 h of treatment in SW1736 cells.

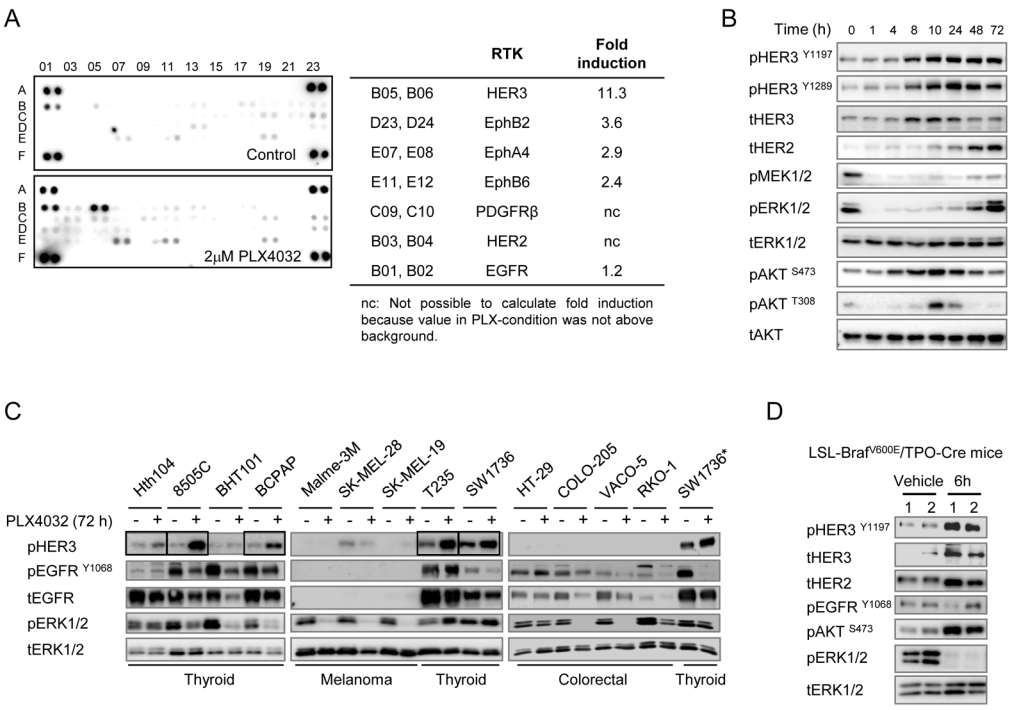

Figure 2.

Phospho-ERK inhibition promotes expression and activation of RTKs in BRAF mutant thyroid cancer cells. **A,** SW1736 cells were left untreated or exposed for 72 h to 2 μM PLX4032 and lysates incubated with phospho-RTK arrays. Spots are in duplicate, with each pair corresponding to a specific pRTK. The pair spots in the corners are positive controls. Comparison between treated and untreated cells demonstrates increased phosphorylation of several RTKs by PLX4032, with pHER3 being the most prominently induced. Normalized data from densitometry analysis of the arrays are listed in the table. **B,** western blots of SW1736 cells treated with 2 μM PLX4032 and collected at the indicated times. Rebound in phospho-ERK and pAKT is associated with induction of total and pHER3, and total HER2. **C,** a panel of 6 thyroid cancer, 3 melanoma and 4 colorectal cell lines with $BRAF^{V600E}$ mutation were treated with or without PLX4032 for 72 h. Immunoblots show an increase of pHER3 in 5/6 thyroid cancer cell lines (SW1736, Hth104, 8505C, BCPAP and T235, see boxes). By contrast, EGFR phosphorylation was lower in 4/6 thyroid cell lines, and unchanged in the others. No comparable induction of pHER3 was observed in melanoma or colorectal cell lines. Lysates of SW1736 were used as an inter-blot control (*). **D,** western immunoblots of thyroid cancer tissue lysates of *TPO-Cre/LSL-*$Braf^{V600E}$ mice treated with a single 25 mg/kg dose of the MEK inhibitor PD0325901 for 6 h. Each lane corresponds to lysates from one mouse thyroid cancer tissue.

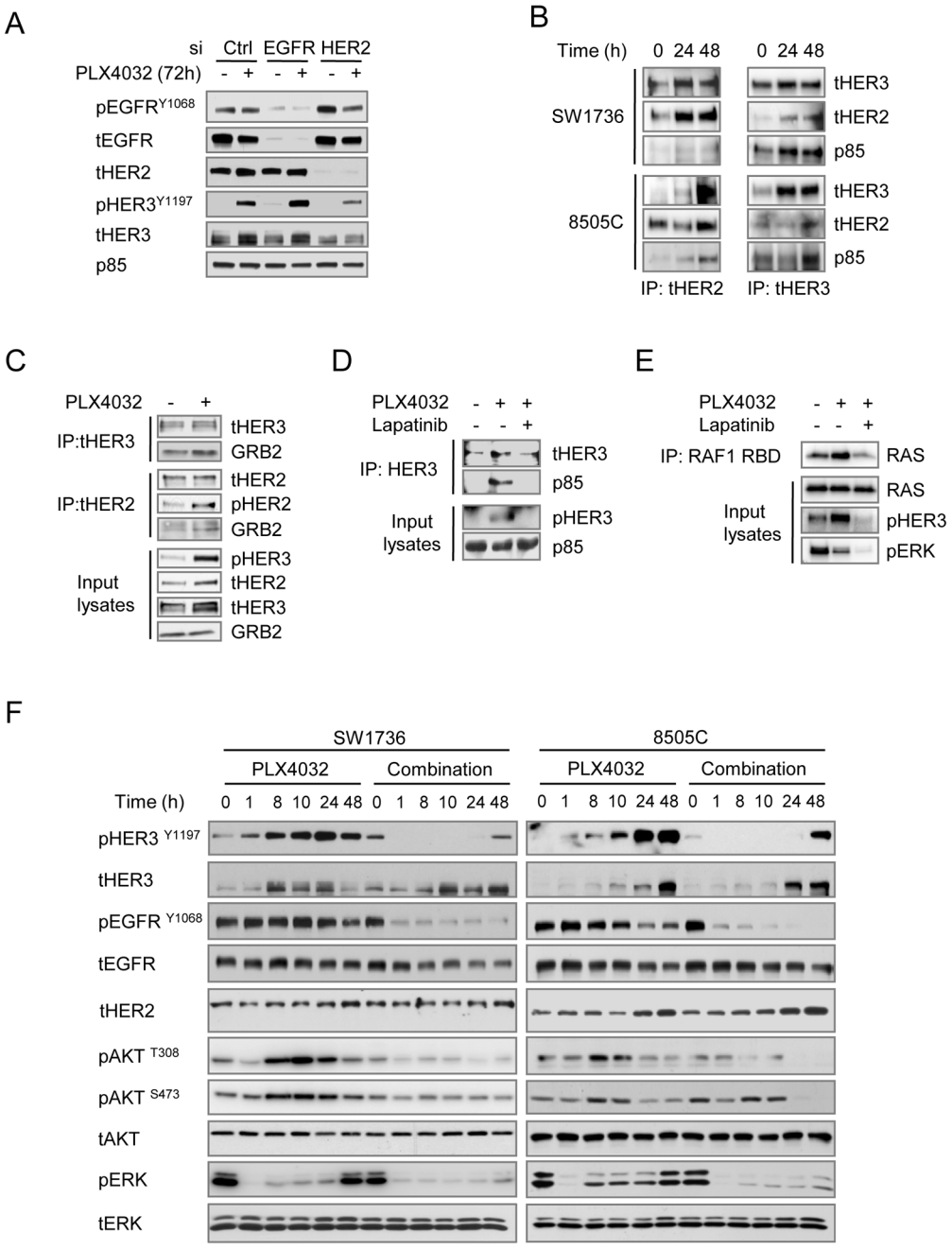

Figure 3.

PLX4032 induces HER2/HER3 heterodimers, recruitment of p85 and activation of RAS. **A,** 8505C cells were transfected with siRNAs against EGFR or HER2, or with a scrambled siRNA control. After 16 h cells were treated with 2 μM PLX4032 for 72 h. Western blotting with the indicated antibodies shows that knockdown of HER2, but not EGFR, reduces PLX4032-induced HER3 phosphorylation. As HER4 was not expressed, RNAi experiments for this RTK were not done. **B,** SW1736 and 8505C cells were treated with 2 μM PLX4032 and collected at 24 and 48 h post-treatment. Lysates were immunoprecipitated with either anti-HER2 or anti-HER3 antibodies and Western blotted for HER3, HER2 or p85. **C,** 8505C cells were treated with 2 μM PLX4032 and collected 72 h post-treatment. Lysates were

immunoprecipitated with either anti-HER3 or anti-HER2 antibodies and Western blotted for HER3, HER2, pHER2 or GRB2. PLX4032-treated cells show increased association of GRB2 to the HER2-HER3 immunocomplex. **D,** 8505C cells were treated with PLX4032 for 22 h and then treated with or without 1 μM lapatinib for 2 h. Lysates were IP with antiHER3 and blotted with the indicated antibodies. **E,** 8505C cells were treated with PLX4032 for 70 h and then incubated with or without 1 μM lapatinib for 2 h. Lysates were immunoprecipitated with RAF-RBD and blotted with the indicated antibodies. PLX4032 treatment induced RAS activation that is blocked by lapatinib. Immunoblotting of the input lysates demonstrates inhibition of pHER3 and pERK1/2 by lapatinib. **F,** western blot of lysates of SW1736 and 8505C cells treated with 2 μM PLX4032 with or without 1 μM lapatinib for the indicated times. Lapatinib blocked the PLX4032-induced HER3 and AKT phosphorylation and the pERK1/2 rebound. EGFR phosphorylation, which was not induced by vemurafenib, was also blocked by lapatinib.

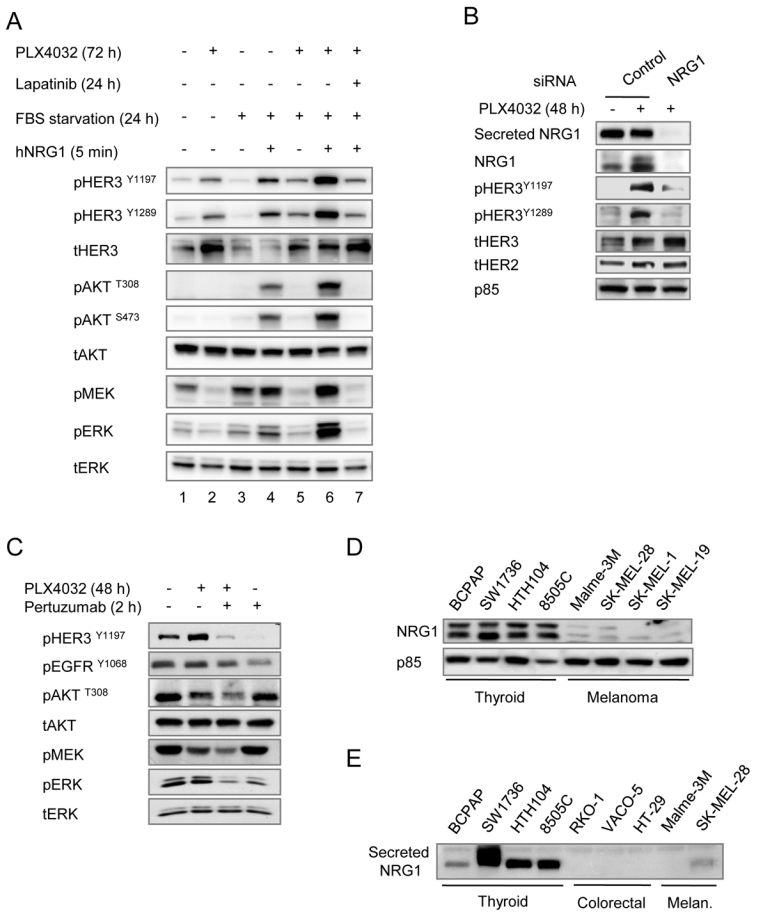

Figure 4.

PLX4032-induced HER2/HER3 activation is dependent on autocrine secretion of Neuregulin-1. **A,** 8505C cells were grown in 10% FBS for 72 h, or for 48 h followed by 24 h in serum free medium, and treated with or without 2 μM PLX4032 for 72 h. Cells in lane 7 were also incubated with 1 μM lapatinib for 24 h. Starved cells were stimulated with the HER3 ligand neuregulin-1 for 5 min. **B,** western blot of lysates or concentrated media of 8505C cells incubated with control or NRG1 siRNA for 60 h and with 2 μM PLX4032 for the final 48 h. Knockdown of NRG1 inhibited the PLX4032-induced HER3 activation. **C,** effects of short term incubation with pertuzumab on PLX4032-induced signaling in 8505C. Addition of 10 μg/ml pertuzumab for 2 h decreased pHER3, pMEK and pERK, with more subtle effects on pT308AKT. Similar findings were seen in SW1736 and Hth104 cells. **D,** endogenous expression of NRG1 in protein lysates of the indicated thyroid cancer and melanoma cell lines. **E,** western immunoblotting for NRG1 of concentrated serum-free media conditioned by the indicated cell lines.

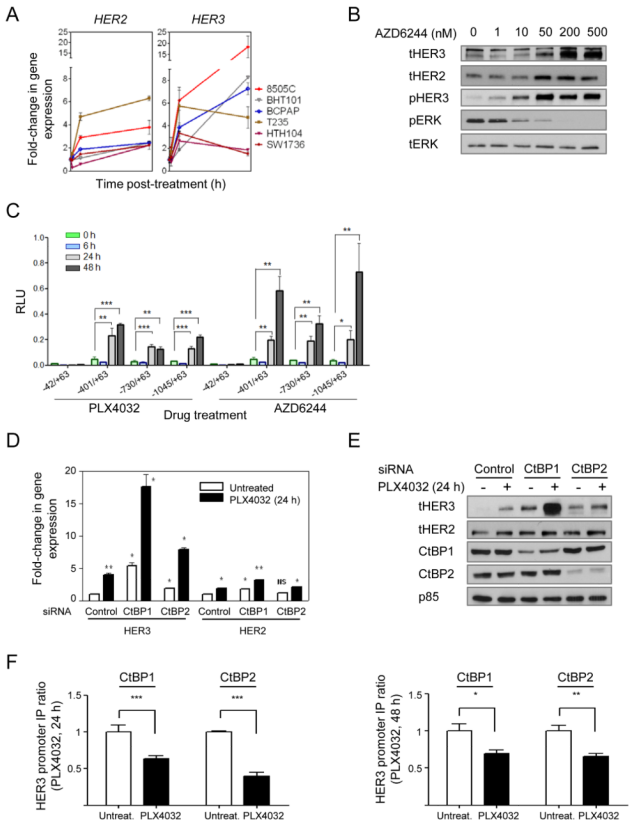

Figure 5.

CtBPs modulate PLX4032 induction of HER3 gene transcription. **A,** a panel of BRAF mutant thyroid cells was treated with 2 μM PLX4032 for 1, 6 or 48 h and cell lysates analyzed for expression of HER3 and HER2 by Q-RT-PCR. Points represent fold-change of HER3/GAPDH Q-RT-PCR values of triplicate assays (mean +/− SD) over untreated controls. **B,** 8505C cells were treated with increasing concentrations of AZD6244. Lysates were extracted at 24 h post-treatment and immunoblotted with the indicated antibodies. **C,** luciferase assays of 8505C cells transfected with plasmids containing HER3 promoter-reporter constructs (−992/+63; −730/+63; −401/+63 or −42/+63, relative to transcriptional start site) and pRenilla-CMV, used as transfection normalizing control plasmid. Twelve hours post-transfection, complete media containing 2 μM PLX4032 or 0.5 μM AZD6244 was added to cells. Lysates were obtained at different time points post-treatment (0, 6, 24 and 48 h), and luciferase activity measured. Promoter activity was determined as the ratio between luciferase and renilla, relative to untreated cells. The results shown are the mean +/− SD of triplicate samples. * $p < 0.05$, ** $p < 0.01$, *** $p < 0.001$. **D,** 8505C cells were transfected with control, CtBP1 or CtBP2 siRNAs and treated with or without 2 μM PLX4032 for 24 h. Lysates were analyzed for expression of *HER3* and *HER2* by RT-PCR. Bars represent mean +/− SD of triplicate assays of HER/GAPDH Q-RT-PCR values relative to untreated controls. **E,** panels show protein levels of HER3, HER2, CtBP1, CtBP2 and p85 (loading control) in cells transfected with control, CtBP1 and CtBP2 siRNAs and grown in either absence or presence of 2 μM PLX4032 for 24 h. **F,** CtBP1 and CtBP2 chromatin immunoprecipitation assays were performed in 8505C cells treated with or without 2 μM PLX4032 for 24 (left) or 48 h (right). A fragment (–246 to –162) of the HER3 promoter that includes known interacting sites for CtBP proteins was amplified by means of RT-PCR for both conditions. Graph shows normalized RT-PCR data of HER3 fragment of the

immunoprecipitated complex compared to input lysate. Data represent mean +/− SD of two independent biological replicates performed in quadruplicate.

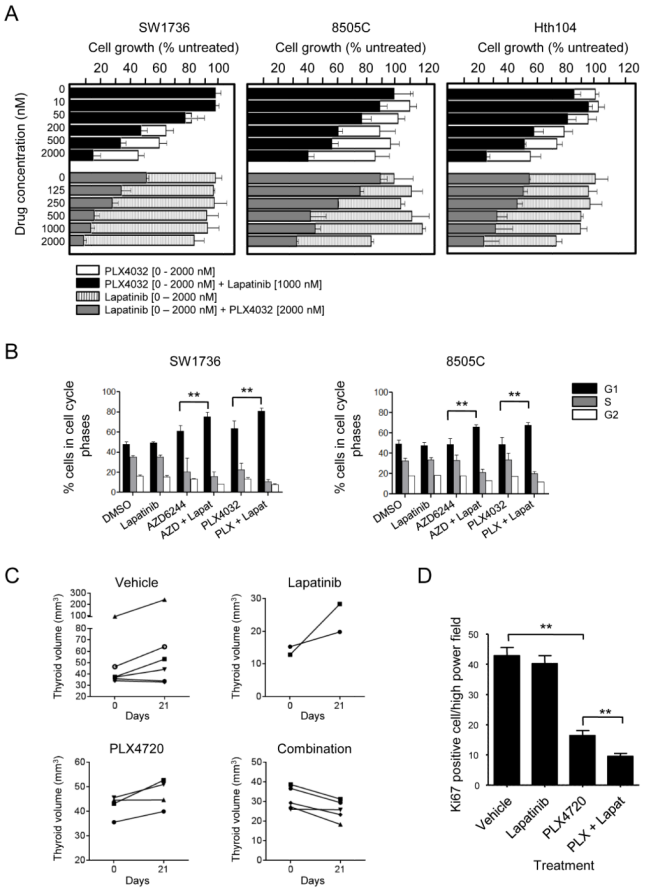

Figure 6.

Lapatinib cooperates with PLX4032 to inhibit BRAF mutant thyroid cancer cell growth. **A,** bars represent growth inhibition of 8505C, SW1736 and Hth104 cells by lapatinib, PLX4032 or their combination. Growth was measured 4 days after addition of the indicated concentration of PLX4032 in the absence (open bars) or presence of 1 μM lapatinib (black), or after addition of the indicated concentration of lapatinib in the absence (hatched) or presence of 2 μM PLX4032 (grey). Bars represent percent change (mean +/− SD) in cell count of triplicate wells compared to untreated cells. **B,** SW1736 and 8505 cells were treated with 2 μM PLX4032, 0.1 μM AZD6244 or 1 μM lapatinib alone or in combination for 48 h. FACS shows a significant increase in G1 phase in cells exposed to PLX4032 or AZD6244 when combined with lapatinib. **C,** Thyroid volumes of *TPO-Cre/LSL-Braf*^{V600E} mice treated with lapatinib (150 mg/kg five times a week), PLX4720-impregnated chow, or their combination at days 0 and 21 of treatment. The fold-change of thyroid volume was significantly lower in mice treated with the combination compared to vehicle (p= 0.02), and PLX4720 alone (p= 0.02). **D,** Bars represent average number of Ki67 positive cells per high power field in mice treated as described above for two weeks, except that lapatinib was given three times a week alone or in combination with PLX4720. At least 8 higher powered fields/section on 4 separate sections were counted for each mouse (2–3 mice per treatment group). **p < 0.01.

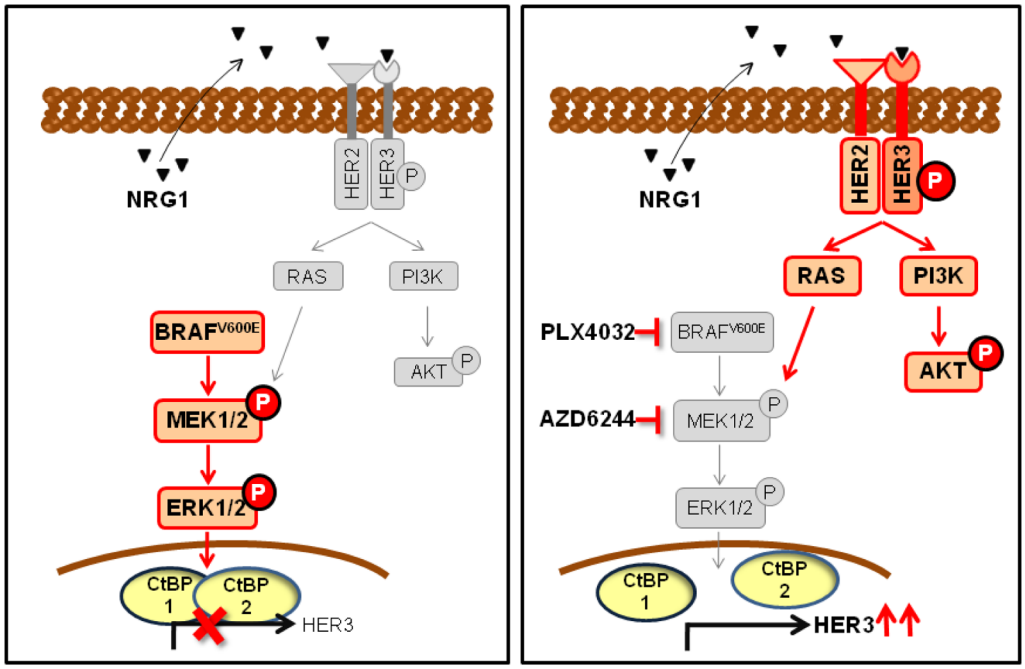

Figure 7.

Model of HER2/HER3-induced primary resistance to MAPK inhibitors in *BRAF* mutant thyroid cancer cells. RAF or MEK inhibitors release transcription repressor CTBP protein/s from the HER3 promoter and induce HER3 gene expression. Autocrine-secreted NRG-1 binds to HER3, triggers HER3/HER2 heterodimerization and receptor phosphorylation, inducing PI3K and reactivating MAPK signaling, thus promoting resistance to growth inhibition.